

Electronic Structures of Oxo-Metal Ions

Jay R. Winkler and Harry B. Gray

Abstract The dianionic oxo ligand occupies a very special place in coordination chemistry, owing to its ability to donate π electrons to stabilize high oxidation states of metals. The ligand field theory of multiple bonding in oxo-metal ions, which was formulated in Copenhagen 50 years ago, predicts that there must be an “oxo wall” between Fe–Ru–Os and Co–Rh–Ir in the periodic table. In this tribute to Carl Ballhausen, we review this early work as well as new developments in the field. In particular, we discuss the electronic structures of beyond-the-wall (groups 9 and 10) complexes containing metals multiply bonded to O- and N-donor ligands.

Keywords Ferryl · Ligand field theory · Oxo wall · Vanadyl

Contents

1	Introduction	18
2	The B&G Bonding Scheme	18
2.1	The Vanadyl Ion	18
2.2	The Chromyl and Molybdenyl Ions	21
2.3	The Oxo-Metal Triple Bond	22
2.4	Lower Bond Orders	22
3	The Oxo Wall	25
4	Beyond the Oxo Wall	26
5	Concluding Remarks	27
	References	28

1 Introduction

Transition metal ions in aqueous solutions typically are coordinated by multiple water molecules. Binding to a Lewis acidic metal center increases the Brønsted acidity of the water ligand such that, depending on the pH of the medium, one or two protons can be lost producing, respectively, hydroxo and oxo ligands. In some cases, the acidity of a coordinated water is so great that the oxo ligand cannot be protonated even in concentrated acid solutions. The short MO bond distances in these oxo complexes (1.6–1.7 Å) are indicative of metal to ligand multiple bonding [1].

Oxo-metal complexes are so pervasive that a unique nomenclature evolved to characterize the structural unit. Koppel and Goldmann in 1903 suggested that aqueous VO^{2+} be known as vanadyl, in analogy to the uranyl ion, and replacing what they viewed as a less consistent term, hypovanadate [2]. Over the ensuing years, oxo complexes of several different metals became known as “-yl” ions. A 1957 IUPAC report on inorganic nomenclature recognized that certain radicals¹ containing oxygen or other chalcogens have special names ending in “-yl”, and the Inorganic Nomenclature Commission in 1957 gave provisional approval to retention of the terms vanadyl (VO^{2+}), chromyl (CrO_2^{2+}), uranyl (UO_2^{2+}), neptunyl (NpO_2^{2+}), plutonyl (PuO_2^{2+}), and americyl (AmO_2^{2+}) [3]. But by 1970, only chromyl and the actinyls were still viewed favorably by IUPAC [4]. The preferred lexical alternative was oxo-metal, wherein O^{2-} is considered as a ligand bound to a metal center. The unfortunate confluence of trivial and systematic names for these compounds leads to abominations such as the resilient “oxoferryl”, a term used all too often to describe complexes containing the FeO^{2+} group.

The electronic structures of oxo-metal complexes were placed on a firm footing in 1962 by Carl Ballhausen (B) and one of us (G) based on experimental and theoretical investigations of the vanadyl ion [5].

2 The B&G Bonding Scheme

2.1 The Vanadyl Ion

Vanadyl complexes are characterized by their rich blue color. Furman and Garner reported one of the earliest spectra of aqueous vanadyl: a single, slightly asymmetric absorption band maximizing at 750 nm ($\epsilon \sim 17 \text{ M}^{-1} \text{ cm}^{-1}$) is the lone feature in the visible region [6]. Measurements reported a year later on complexes of the vanadyl ion with thiocyanate revealed that the asymmetry is due to a second

¹IUPAC defined a radical as a group of atoms which occurs repeatedly in a number of different compounds.

absorption feature: a shoulder at ~650 nm in vanadyl sulfate; a resolved 560 nm maximum in the SCN^- complex [7].

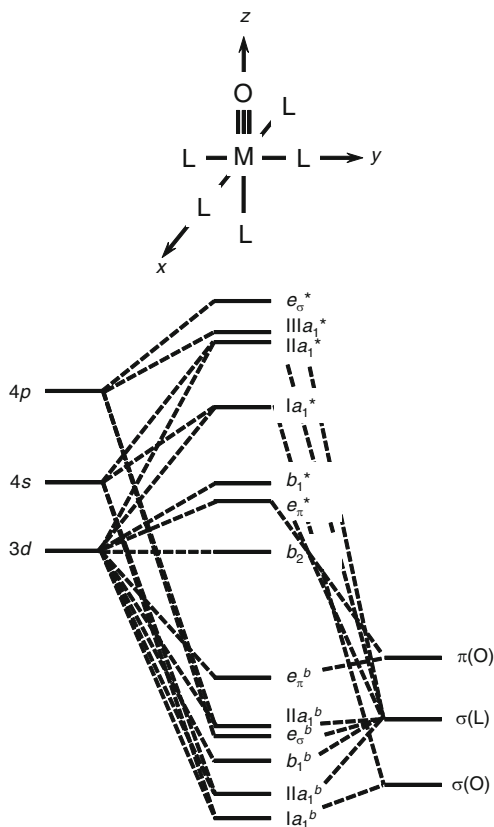
Jørgensen first used crystal field (CF) theory to explain the absorption spectrum of the aqueous vanadyl ion, its complexes with donor ligands (edta, oxalate, acetylacetonate, and tartrate), as well as that of molybdenyl chloride (MoOCl_5^{2-}) [8]. Importantly, the spectra of the edta and tartrate complexes exhibit a third weak band maximizing in the 25,000–30,000 cm^{-1} range ($\epsilon < 50 \text{ M}^{-1} \text{ cm}^{-1}$). He recognized that the octahedral CF-splitting parameter for V^{4+} should be ~25,000 cm^{-1} : the bands at 13,100 and 16,000 cm^{-1} in the VO^{2+} spectrum are at much lower energies than expected for transitions derived from $t_{2g} \rightarrow e_g$ parentage. Jørgensen suggested that the 25,000–30,000 cm^{-1} bands in $\text{VO}(\text{edta})^{2-}$ and $\text{VO}(\text{tart})^{2-}$ are in better agreement with this transition. His analysis treated the $d^1 \text{VO}^{2+}$ complexes as tetragonally Jahn–Teller distorted cubic complexes, analogous to $d^9 \text{Cu}^{2+}$ ions but with axial compression rather than elongation. The limiting Jahn–Teller distortion in vanadyl complexes would produce the diatomic VO^{2+} ion [8].

In 1962, B&G developed a molecular orbital energy level scheme to describe the absorption and electron paramagnetic resonance spectra of the vanadyl ion [5]. The VO^{2+} molecular orbital splitting pattern (Fig. 1) is reminiscent of the CF analysis put forth by Jørgensen, but it is important to emphasize that a pure CF model without oxo-metal π bonding cannot provide an adequate description of the vanadyl electronic structure. The B&G MO model provides remarkably accurate predictions of the energy, intensity, and polarization of the absorption features in the vanadyl spectrum, as well as the g -values extracted from EPR spectra. The key feature of the model is the substantial destabilization of the degenerate $d_{xz,yz}$ orbital pair, owing to π -bonding with the oxo-ligand. The lowest energy absorption feature (~13,000 cm^{-1}) was attributed to the ${}^2\text{B}_2(xy) \rightarrow {}^2\text{E}(xz,yz)$ excitation, corresponding to promotion of an electron from a nonbonding to the VO π -antibonding orbital. That the energy of the ${}^2\text{B}_2(xy) \rightarrow {}^2\text{E}(xz,yz)$ transition in VO^{2+} is nearly as great as that of the $t_{2g} \rightarrow e_g$ excitation in $\text{Ti}(\text{OH}_2)_6^{3+}$ [9, 10] emphasizes the importance of VO π -bonding. The shoulder at ~16,000 cm^{-1} arises from the ${}^2\text{B}_2(xy) \rightarrow {}^2\text{B}_1(x^2 - y^2)$ transition and provides a direct estimate of the octahedral ligand field splitting parameter (10Dq). For comparison, 10Dq values for the V^{2+} [10, 11] and V^{3+} [10, 12–14] hexaaqua ions are estimated to be ~12,000 and 18,800 cm^{-1} , respectively. The absorption spectrum reveals that the strength of the $\text{V-OH}_{2(\text{equatorial})}$ interaction in the vanadyl ion lies somewhere between that of V^{2+} and V^{3+} .

Particularly noteworthy is the finding that the VO^{2+} absorption spectrum is unaffected by changes in pH from –0.5 to 1.5 [15]. The extremely low pKa of VO^{2+} is a direct consequence of strong VO π -bonding: two oxygen $2p$ orbitals are used for π -bonds to V(IV) and only a nonbonding sp_σ hybrid orbital remains for interaction with a proton. The energy of the hybrid orbital, with its substantial $2s$ character, is poorly suited to bonding with H^+ .

It is curious that the aqueous vanadyl ion is $\text{VO}(\text{OH}_2)_5^{2+}$ rather than $\text{V}(\text{OH})_2(\text{OH}_2)_4^{2+}$. Indeed, Jørgensen considered these and other isomers in his

Fig. 1 B&G molecular orbital model of the electronic structures of tetragonal oxo-metal complexes



analysis of the vanadyl spectrum [8]. Taube attributed the formation of -yl ions to the fact that the Lewis acidic metal center exerts a selective polarization of the surrounding water molecules, leading to double deprotonation of one water ligand rather than single deprotonation of two waters [16]. He argued that -yl ion formation is a consequence of the polarizability of O^{2-} , which is substantially greater than that of HO^- . The equivalent statement in the B&G molecular orbital language is that O^{2-} is a far stronger π -donor than HO^- such that the net stabilization gained by forming two π -bonds to one O^{2-} ligand is greater than that resulting from one π -bond to each of two HO^- ligands.

A minor controversy surrounding the B&G model developed in late 1963 with the publication by Selbin and coworkers of the spectrum of $VO(acac)_2$ dissolved in organic glasses at 77 K [17]. At cryogenic temperature the absorption bands narrowed, lost some intensity, and the lowest energy feature resolved into three distinct maxima. The authors attributed the four bands observed between 12,000 and 18,000 cm^{-1} to the four distinct ligand field excitations expected for a d^1 complex with C_{2v} symmetry. Workers in Copenhagen addressed this issue in 1968 with X-ray and optical spectroscopic measurements on crystalline $VO(SO_4) \cdot 5H_2O$ [18]. An improved X-ray crystal structure determination and low temperature

(20 K) single-crystal absorption spectra provided convincing evidence in support of the original B&G assignments. It is likely that the additional peaks observed by Selbin in the 77 K spectrum of VO(acac)₂ arise from vibrational fine structure in the VO stretching mode (*vide infra*). Such a progression is indicative of a distortion in the VO bond, consistent with the B&G $n \rightarrow \pi^*(\text{VO})$ assignment.

2.2 The Chromyl and Molybdenyl Ions

Three months after the B&G analysis of the vanadyl electronic structure appeared in *Inorganic Chemistry* [5], Curt Hare (H) and one of us (G) published an interpretation of chromyl (CrOCl_5^{2-}) and molybdenyl (MoOCl_5^{2-}) spectra and electronic structures [19]. The assignments parallel those for the vanadyl ion: the lowest energy feature (CrO^{3+} , 12,900 cm^{-1} ; MoO^{3+} , 13,800) is attributed to the ${}^2\text{B}_2(xy) \rightarrow {}^2\text{E}(xz, yz)$ transition; the next higher energy band (CrO^{3+} , 23,500 cm^{-1} ; MoO^{3+} , 23,000) is ${}^2\text{B}_2(xy) \rightarrow {}^2\text{B}_1(x^2 - y^2)$. It is interesting to note that although the lowest energy bands in CrO^{3+} and MoO^{3+} are about the same position as the corresponding feature in the VO^{2+} spectrum, the second band is some 5,000–7,000 cm^{-1} higher energy in the group 6 ions. The energy of the second band provides a direct estimate of 10Dq. This ligand field splitting parameter for the molybdenyl ion is nearly identical with that of MoCl_6^- [20, 21], and about 4,000 cm^{-1} greater than that of MoCl_6^{3-} [10], as expected for the higher oxidation state metal.

Garner and coworkers cast doubt on the ${}^2\text{B}_2(xy) \rightarrow {}^2\text{B}_1(x^2 - y^2)$ assignment for the 23,000 cm^{-1} band in MoOCl_5^{2-} [22]. Calculations placed the ${}^2\text{B}_2(xy) \rightarrow {}^2\text{E}(xz, yz)$ and ${}^2\text{B}_2(xy) \rightarrow {}^2\text{B}_1(x^2 - y^2)$ transitions at 15,600 and 23,000 cm^{-1} , but indicated that absorption corresponding to the latter transition would be obscured by $\pi\text{Cl} \rightarrow \text{Mo}$ charge-transfer features. We addressed this controversy with measurements of the spectra of $\text{MoO}(\text{HSO}_4)_4^-$ and $\text{MoO}(\text{H}_2\text{PO}_4)_4^-$: both ions exhibit weak ($\epsilon < 30 \text{ M}^{-1} \text{ cm}^{-1}$) absorptions at 14,000 and 26,000 cm^{-1} that are assigned to ${}^2\text{B}_2(xy) \rightarrow {}^2\text{E}(xz, yz)$ and ${}^2\text{B}_2(xy) \rightarrow {}^2\text{B}_1(x^2 - y^2)$ transitions, respectively [23]. With the exception of a 2,000–3,000 cm^{-1} blue shift in the second band, consistent with the stronger ligand field expected for O-donating equatorial ligands, the spectra match that of MoOCl_5^{2-} quite closely. It is unlikely, then, that the 23,000 cm^{-1} band in the latter complex is due to $\text{Cl} \rightarrow \text{Mo}$ charge transfer. Indeed, the spectra of $\text{MoO}(\text{HSO}_4)_4^-$ and $\text{MoO}(\text{H}_2\text{PO}_4)_4^-$ place a lower limit (35,000 cm^{-1}) on the energy of $\pi\text{O} \rightarrow \text{Mo}$ charge transfer in molybdenyl ions. It follows that bands observed at 28,000 and 32,500 cm^{-1} in MoOCl_5^{2-} likely arise from $\pi\text{Cl} \rightarrow \text{Mo}$ charge transfer.

Low-temperature (5 K) single-crystal polarized absorption spectra of $(\text{Ph}_4\text{As})[\text{MoOCl}_4]$ exhibit rich vibrational fine structure in both ${}^2\text{B}_2(xy) \rightarrow {}^2\text{E}(xz, yz)$ and ${}^2\text{B}_2(xy) \rightarrow {}^2\text{B}_1(x^2 - y^2)$ absorption systems [23]. The ${}^2\text{B}_2 \rightarrow {}^2\text{E}$ band is characterized by progressions in 900 and 165 cm^{-1} : the high-frequency progression corresponds to the MoO stretching mode in the ${}^2\text{E}$ excited state; and the 100 cm^{-1}

reduction in frequency relative to the ground state is consistent with population of a MoO π^* orbital. Franck–Condon analysis of the absorption profile is consistent with a 0.09(1) Å distortion of the MoO bond in the 2E state. Vibrational progressions in MO stretching modes, sometimes apparent even at room temperature in fluid solutions, are diagnostic of $(xy) \rightarrow (xz, yz)$ excitations in tetragonal oxo-metal complexes. The lower frequency vibrational progression was originally attributed to the symmetric OMoCl umbrella bending mode, but later work on related complexes suggests that the $b_1(\text{OMoCl})$ bend is a better assignment [24]. Vibrational fine structure in the $^2B_2(xy) \rightarrow ^2B_1(x^2 - y^2)$ system corresponds to the symmetric MoCl stretch and Franck–Condon analysis suggests a 0.07(1) Å distortion along each MoCl bond in the 2B_1 excited state.

A final point of interest is the finding that molybdenyl ions are luminescent [25–27]. Crystalline samples of $(\text{Ph}_4\text{As})[\text{MoOX}_4]$ ($X=\text{Cl}, \text{Br}$) exhibit emission maxima at ~ 900 nm, and at cryogenic temperatures a progression in the MoO stretching mode is resolved [27]. The luminescence lifetime of $(\text{Ph}_4\text{As})[\text{MoOCl}_4]$ is 160 ns at room temperature, increasing to 1.4 μs at 5 K, but no luminescence from this molybdenyl ion could be detected in fluid solutions or frozen glasses. Using the Strickler–Berg approximation [28] to estimate the radiative decay rate constant for the $^2B_2(xy) \rightarrow ^2E(xz, yz)$ transition, a room temperature quantum yield of ~ 0.01 can be extracted for crystalline $(\text{Ph}_4\text{As})[\text{MoOCl}_4]$.

2.3 The Oxo-Metal Triple Bond

G&H were the first to represent the interaction between the molybdenum and oxygen atoms in MoO^{3+} as a triple bond ($\text{M}\equiv\text{O}$) [19]. This assignment of bond order follows directly from the molecular orbital model of the electronic structure: two electrons in a MO σ -bonding orbital; and four electrons in a doubly degenerate pair of MoO π -bonding orbitals. The lone electron in the $b_2(xy)$ orbital is nonbonding with respect to the MO interaction. The triple bond ($\text{M}\equiv\text{O}$) is the proper formulation of electronic structures in d^0 , d^1 , and d^2 (low spin) tetragonal monooxo-metal complexes. It is distressing to see the MO interaction in these cases represented as a double bond, likely by those who think (incorrectly) that it is analogous to the double bond in organic carbonyl complexes. But, just as carbon monoxide possesses a triple bond, so do VO^{2+} , CrO^{3+} , MoO^{3+} , and WO^{3+} . Metal nitrido complexes also feature strong MN multiple bonding: indeed, d^0 , d^1 , and d^2 (low spin) tetragonal nitrido-metal complexes all contain MN triple bonds ($\text{M}\equiv\text{N}$).

2.4 Lower Bond Orders

Population of $e(xz, yz)$ π^* orbitals in tetragonal oxo-metal complexes reduces the MO bond order. Although triple bonding is assured in d^0 and d^1 complexes, the

bond order in complexes with two or three d -electrons depends critically on the spin state (Fig. 2). Tetragonal monooxo-complexes with d^2 configurations have MO bond orders of 3 and 2.5 in the low-spin (1A_1) and high-spin (3E) states, respectively. For d^3 configurations, the bond orders are 2.5 (2E) and 2 (4B_1). The relative energies of high- and low-spin states depend on a balance between the $e(xz,yz) - b_2(xy)$ energy gap (Δ_π) and the electron–electron repulsion energies. This relationship can be represented graphically with modified Tanabe–Sugano (TS) diagrams [29, 30] (Fig. 3). Owing to differences in MO bond lengths in the high- and low-spin states, there is a “forbidden region” of the TS diagram (Fig. 3, gray area) that excludes a range of Δ_π values for ground states. Taking typical values for Racah parameters ($B = 500 \text{ cm}^{-1}$, $C/B = 4$), we find that the $^3E-^1A_1$ spin crossover occurs with $\Delta_\pi \sim 9,500 \text{ cm}^{-1}$ in d^2 oxo-metal complexes, but formation of a low-spin ground state requires $\Delta_\pi > 13,000 \text{ cm}^{-1}$. This value of Δ_π is about the same as that found in the d^1 -yl ions, suggesting that d^2 oxo and nitrido-metal complexes are likely to have low-spin (1A_1) ground states, but that high-spin complexes might be thermally accessible. It is important to remember that the TS diagrams represent vertical energy differences [31]; the energy required for thermal population of a high-spin state in d^2 complexes will be less than the vertical energy difference by several thousand wavenumbers. A larger $e(xz,yz) - b_2(xy)$ energy gap is required to produce low-spin d^3 oxo-metal complexes; the $^2E-^4B_1$ spin crossover occurs at $\Delta_\pi \sim 13,000 \text{ cm}^{-1}$, but $\Delta_\pi > 17,000 \text{ cm}^{-1}$ is required for a low-spin ground state.

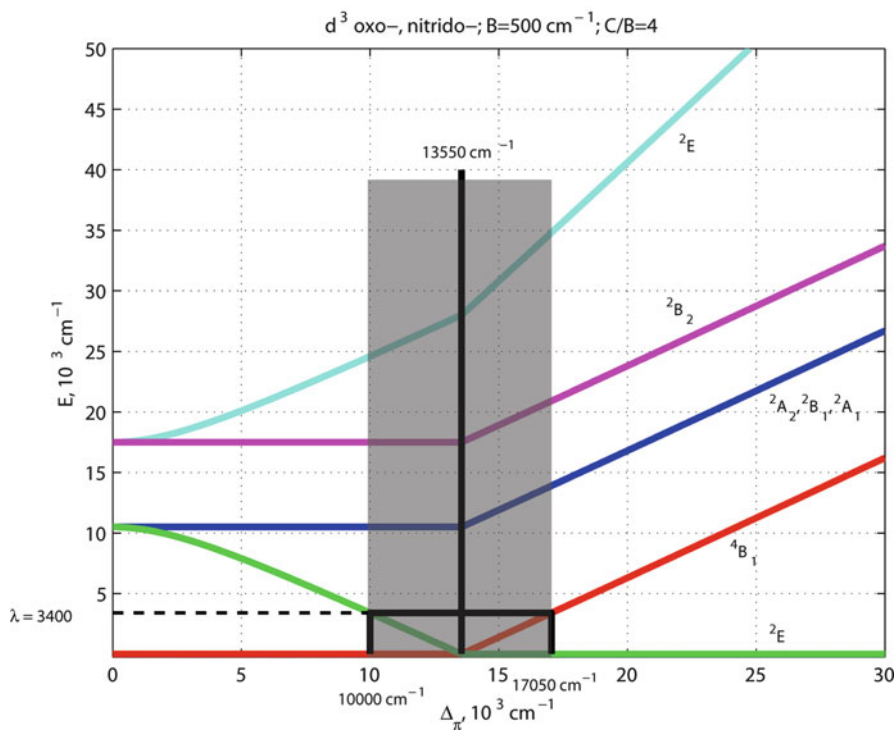
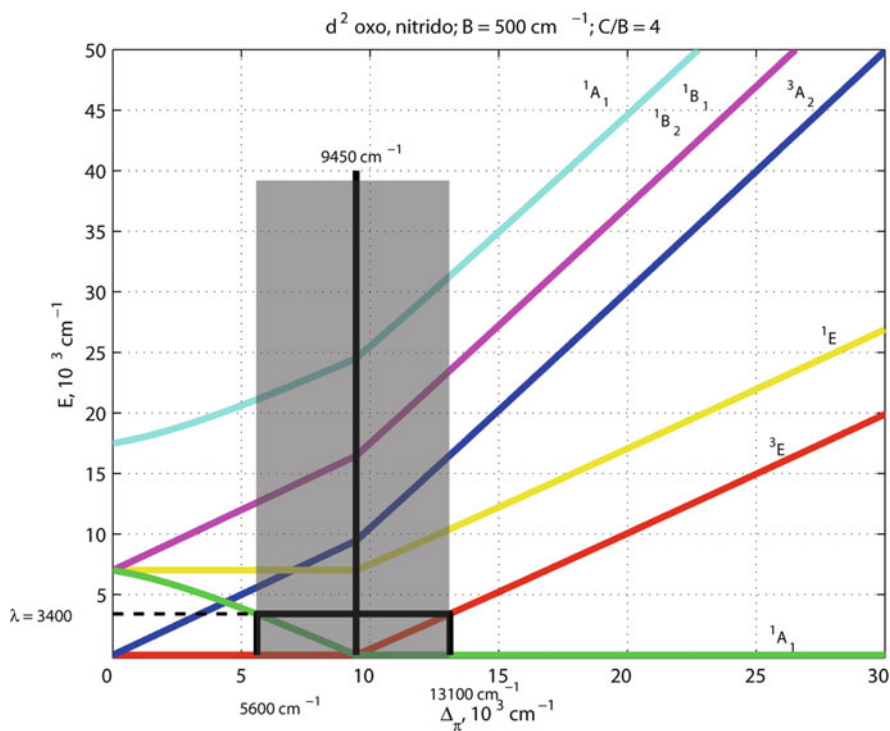
d Count Bond Order	d^0	d^1	d^2	d^3	d^4	d^5
3 M≡O	— — — — —	— — — — ↑	— — — — ↑↓	— — — — —	— — — — —	— — — — —
2.5 M≡O	— — — — —	↑ — — — —	↑ — — — ↑	↑ — — — ↑↓	— — — — —	— — — — —
2 M=O	— — — — —	— — — — —	↑ — — — —	↑ — — — ↑	↑ — — — ↑↓	— — — — —
1.5 M≡O	— — — — —	— — — — —	— — — — —	↑ — — — —	↑ — — — ↑	↑ — — — ↑↓

Ground State

First Excited State

Higher Excited State

Fig. 2 Correlation of MO bond order with d -electron count in oxo-metal complexes. The gray shaded region corresponds to a π bond order of 0.5; the oxo ligands in these complexes are expected to be extremely basic



Substantially stronger ME π -bonding ($E=O$, N) is required to produce low-spin ground states in d^3 than in d^2 complexes. Nitrido ligands are stronger π donors than oxo ligands; ligand field theory predicts that the ground state in d^3 tetragonal oxo-metal complexes will be 4B_1 (high spin), whereas nitrido complexes of this electronic configuration are more likely to have 2E (low-spin) ground states. Rounding out the possible oxo-metal configurations, most tetragonal d^4 oxo-metal complexes have a 3A_2 ground state and MO bond order of 2, whereas d^5 complexes have a bond order of 1.5. In some ferryl (d^4) complexes with very weak equatorial ligand fields, the x^2-y^2 orbital drops in energy, producing an $S = 2$ ground state (e.g., $^5(Fe=O)^{2+}$), but retaining an MO bond order of 2 [32–34].

In tetragonal *trans*-dioxometal complexes with 0, 1, or 2 d -electrons, 4 bonds (two σ and two π) will be divided between two MO interactions. The average MO bond order is two, such that a double bond representation is not incorrect, although a structure with one full bond and two half bonds is a more accurate depiction of the interaction.

3 The Oxo Wall

The B&G bonding model defines electronic structural criteria for the existence of oxo-metal complexes. Complexes with tetragonal symmetry can have no more than 5 d -electrons and still retain some MO multiple bonding. In the absence of π -bonding to the metal, the oxo will be extremely basic and unstable with respect to protonation or attack by electrophiles. Achieving the low d -electron counts necessary for MO multiple bonding becomes increasingly difficult for metals on the right half of the transition series. Eventually, the metal oxidation states required for oxo formation become so great that the complexes are unstable with respect to elimination of H_2O_2 or O_2 . The combined requirements of low d -electron counts and limiting metal oxidation states erect an “oxo wall” between groups 8 and 9 in the periodic table (Fig. 4). To the right of this wall, tetragonal oxo complexes are not likely to be found. Hence, while iron, ruthenium, and osmium form -yl complexes, the same cannot be said for cobalt, rhodium, and iridium.

Fig. 3 TS-type diagrams correlating the energies of electronic states in d^2 and d^3 oxo-metal complexes with the strength of the Δ_π ligand field splitting parameter. Gray areas correspond to forbidden Δ_π zones for ground-state complexes

But, mixing with the 4s level produces a d_{z^2} -s hybrid orbital with reduced density along the axis and increased density in the doughnut-shaped lobe in the equatorial plane that is devoid of ligands. The low coordination number in the molecule leads to z^2 -s hybridization, allowing strong NiNR π bonding.

5 Concluding Remarks

Realistic targets that would constitute B&G approved oxo-wall violations include tetragonal *trans*-dioxo Ir(VII) complexes. Josh Palmer, a recent member of our research group, made several unsuccessful attempts to prepare such (and related nitrido) species.

As we approach the 50th anniversary of the publication of the B&G bonding model, inorganic chemists still have not found a stable tetragonal oxo complex of a group 9 or 10 metal!

Acknowledgments We dedicate this paper to the memory of Carl Ballhausen, a great scientist and a dear friend (Fig. 5). We note in closing that the B&G model is providing a firm foundation for structure/reactivity correlations in our current work on oxo-metal complexes [oxidative



Fig. 5 Carl Ballhausen visited the Beckman Institute at Caltech on several occasions. This photograph from one visit in the early 1990s shows (left to right): Gary Mines, Jay Winkler, Bo Malmström, Harry Gray, Carl Ballhausen, Danilo Casimiro, I-Jy Chang, Jorge Colón, Zhong-Xian Huang, and Deborah Wuttke

enzymes P450 and nitric oxide synthase (NIH DK019038, GM068461); water oxidation catalysts (NSF CCI Solar Program, CHE-0947829); and *trans*-dioxo osmium(VI) electrochemistry and photochemistry (BP)]. We thank the Gordon and Betty Moore Foundation and the Arnold and Mabel Beckman Foundation for support of our research programs.

References

1. Nugent WA, Mayer JM (1988) Metal-ligand multiple bonds. John Wiley & Sons, New York
2. Koppel J, Goldmann R (1903) *Z Anorg Allg Chem* 36:281
3. International Union of Pure and Applied Chemistry (1960) *J Am Chem Soc* 82:5523
4. International Union of Pure and Applied Chemistry (1970) Nomenclature of inorganic chemistry. Butterworths, London
5. Ballhausen CJ, Gray HB (1962) *Inorg Chem* 1:111
6. Furman SC, Garner CS (1950) *J Am Chem Soc* 72:1785
7. Furman SC, Garner CS (1951) *J Am Chem Soc* 73:4528
8. Jørgensen CK (1957) *Acta Chem Scand* 11:73
9. Hartmann H, Schlafer HL (1954) *Angew Chem Int Ed Engl* 66:768
10. Ballhausen CJ (1962) Introduction to ligand field theory. McGraw-Hill, New York
11. Bennett RM, Holmes OG (1960) *Can J Chem* 38:2319
12. Hartmann H, Schlafer HL (1951) *Z Naturforsch A* 6:754
13. Hartmann H, Schlafer HL (1951) *Z Naturforsch A* 6:760
14. Ilse FE, Hartmann H (1951) *Z Naturforsch A* 6:751
15. Rossotti FJC, Rossotti HS (1955) *Acta Chem Scand* 9:1177
16. Taube H (1982) In: Rorabacher DB, Endicott JF (eds) *Mechanistic Aspects of Inorganic Reactions*, vol 198, ACS Symposium Series. American Chemical Society, Washington DC, p 151
17. Selbin J, Ortolano TR, Smith FJ (1963) *Inorg Chem* 2:1315
18. Ballhausen CJ, Djurinski BF, Watson KJ (1968) *J Am Chem Soc* 90:3305
19. Gray HB, Hare CR (1962) *Inorg Chem* 1:363
20. Patterson HH, Nims JL (1972) *Inorg Chem* 11:520
21. Horner SM, Tyree SY (1963) *Inorg Chem* 2:568
22. Weber J, Garner CD (1980) *Inorg Chem* 19:2206
23. Winkler JR, Gray HB (1981) *Comments Inorg Chem* 1:257
24. Hopkins MD, Miskowski VM, Gray HB (1986) *J Am Chem Soc* 108:6908
25. Mohammed AK, Fronczek FR, Maverick AW (1994) *Inorg Chim Acta* 226:25
26. Mohammed AK, Maverick AW (1992) *Inorg Chem* 31:4441
27. Winkler JR (1984) *Spectroscopy and Photochemistry of Metal-Oxo Complexes*, Ph.D. California Institute of Technology, California
28. Strickler SJ, Berg RA (1962) *J Chem Phys* 37:814
29. Tanabe Y, Sugano S (1954) *J Phys Soc Jpn* 9:753
30. Tanabe Y, Sugano S (1954) *J Phys Soc Jpn* 9:766
31. Winkler JR, Rice SF, Gray HB (1981) *Comments Inorg Chem* 1:47
32. Sinnecker S, Svensen N, Barr EW, Ye S, Bollinger JM Jr, Neese F, Krebs C (2007) *J Am Chem Soc* 129:6168
33. Riggs-Gelasco PJ, Price JC, Guyer RB, Brehm JH, Barr EW, Bollinger JM, Krebs C (2004) *J Am Chem Soc* 126:8108
34. Price JC, Barr EW, Tirupati B, Bollinger JM, Krebs C (2003) *Biochemistry* 42:7497
35. Hay-Motherwell RS, Wilkinson G, Hussain-Bates B, Hursthouse MB (1993) *Polyhedron* 12:2009
36. Poverenov E, Efremenko I, Frenkel AI, Ben-David Y, Shimon LJW, Leituss G, Konstantinovskii L, Martin JML, Milstein D (2008) *Nature* 455:1093
37. Laskowski CA, Miller AJM, Hillhouse GL, Cundari TR (2011) *J Am Chem Soc* 133:771

Molecular Electronic Structures of Transition Metal
Complexes I

Mingos, D.M.P.; Day, P.; Dahl, J.P. (Eds.)

2012, XVI, 216 p., Hardcover

ISBN: 978-3-642-27369-8